Automated Measurement Procedure for the Calibration of Planar Active Arrays

M. A. Salas Natera, R. Martínez Rodríguez-Osorio and L. de Haro Ariet

Dpto. Señales, Sistemas y Radiocomunicaciones. Universidad Politécnica de Madrid
ETSI de Telecomunicación, Ciudad Universitaria, 28040, Madrid, Spain.
{msalasn; ramon; leandro}@gr.ssr.upm.es

***Abstract*— This work has been focused to describe the development and implementation of an automated system for measurement, characterization of planar active arrays. This automated system is capable of reducing time and operative cost and it is based on multilayer hardware architecture and control software. The system has been tested on one triangular active array panel of the Geodesic Antenna Array (GEODA) which is part of an R & D project to incorporate active antenna arrays into the ground segment for meteorological satellite communication. The measurements and characterization are important, complicated and multipart tasks in the design, development and calibration of active antenna arrays.**

I. INTRODUCTION

Nowadays, earth station which integrate the ground segment have as a common feature, the use of large reflector antenna for downloading data from satellites [1]. However, these large dishes pose a number of impairments regarding their mechanical complexity, low flexibility, and high cost. Furthermore, with the launch of several new satellites, the capacity of existing earth station will be saturated [2][3]. As a consequence, the feasibility of other antenna technologies must be evaluated, such as conformal adaptive antennas based on multiple planar active arrays like geodesic antenna array.

Antenna arrays have several advantages over large dishes: the capability to track several satellites simultaneously, higher flexibility, lower production and maintenance cost, modularity and a more efficient use of the spectrum are the most important of their advantages. In this work the antenna under test (AUT) is a planar active array as a part of one geodesic adaptive antenna GEODA, which has been designed as a first version to receive signals at 1.7 GHz. Subsequently, in recent efforts the GEODA system has been upgraded also for transmission [4]. This antenna uses adaptive beamforming algorithms based on spatial reference to track LEO satellites. The computation of a close approach of the direction of arrival (DoA) and the correct performance of the beamformer depends on the calibration procedure implemented.

Since the AUT is an active array there are static and dynamic errors due to manufacturing and gradual changes as a result of the thermal variation and the aging of components. Fig. 1 shows a categorization of these errors, where SMC, SLE, SGE and SPE are the Sensor Mutual Coupling, Sensor Location, Sensor Gain, Sensor Phase Errors, respectively, of the static group; and SAE, SPSE and STE are the Sensor Amplifier, Sensor Phase Shifter and Sensor Temperature Error, respectively, of the dynamic group. In order to compensate the degradation due to these errors, intensive calibration techniques must be implemented.

Fig. 1 Categorization of the active phased array

In addition to static and dynamic errors to be considered at the Off-line and On-line calibration procedure in Fig. 2, an On-site calibration process is added to compensate the change due to the work frequency for transmission. The goal of the On-site calibration process is to compensate the static errors with a calibration model valid for uplink frequency. Therefore, the AUT measurement requirements are those owing to the Off-line, On-line and On-site calibration procedure.

In this work, we present a measurement procedure for active antenna arrays capable of reducing time and operative cost based on an automation system with multilayer hardware architecture.

The paper is organized as follows. Section II introduces the antenna under test. Section III describes the control system of the AUT. Section IV explains the measurement procedure. Section V presents a discussion about the more relevant results. Finally, section VI draws the conclusions of this paper.

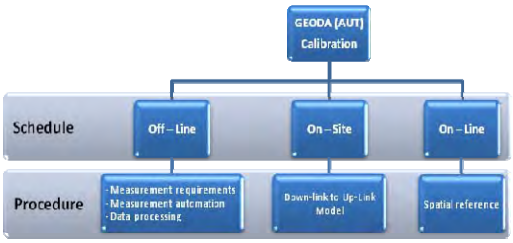

Fig. 2 Calibration procedure for the AUT

II. THE ANTENNA UNDER TEST

For this contribution the AUT is one conformal adaptive antenna based on multiple planar active arrays as geodesic antenna array (GEODA). This antenna is a candidate for a new generation of ground stations for satellites

communications [5]. The antenna has two geometrical structure parts. The first one, is based on a cylinder conformed by 30 triangular planar active arrays (panel), and the second is a half dodecahedron geodesic dome conformed by 30 triangular planar active arrays, as is presented in Fig. 3. Each triangular array is composed by 45 elements as double stacked circular patches with their own RF circuit. There are 15 sub-arrays (cells) with 3 elements. In total there are 45x(30+30) radiating elements each with its active RF section.

The RF circuit of each cell is composed of one hybrid coupler with a 25dB test signal coupler added for calibration purposes, an LNA with 3 states (on, off, bypass) and one phase shifter with 6 states per patch. The outputs of the 3 patches are combined into one signal using a Wilkinson combiner. This signal is amplified with another LNA at the output of the cell [5].

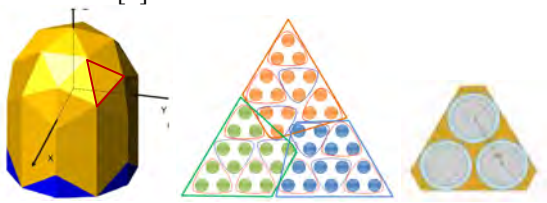

Fig. 3 Antenna structure, planar active array and sub-array

III. Control System

The control system has two main parts: the hardware structure and the control system software. A three-layers architecture has been implemented for the hardware structure. The first layer consist of one embedded microcontroller in each cell RF circuit which controls the phase shifter, the LNA and the test signal coupler switch. The second layer has a main board with one embedded microcontroller which manages the control data address to each cell. The third layer is the work station PC which controls and manages the data control sent to the antenna. The control system software named GCS (GEODA Control System) manages one panel for its measurement, characterization and calibration. The GCS controls four tasks: satellite tracking, anechoic chamber measurements, S21 measurement of the RF circuit and the S21 measurement with the test signal for RF calibration.

IV. Measurement Procedure

To achieve the requirements, here is presented a measurement procedure with four groups of tests that must be executed as a sequence.

A. S21parameter of the RF circuits measurement

This test requires more than 1600 different measurements per triangular active array considering all combination of LNA and phase shifter states. The implemented automated procedure reduces measurement time from the 7 hours of conventional procedures to 8 minutes.

B. S coupling parameter measurement

The active pattern of each patch is obtained by one exhaustively S coupling parameter measurement of the 45 ports of the panel. Measurement results are used to develop a mutual coupling calibration model for the antenna.

C. Test signal of the RF circuit

The test signal is injected through the 25 dB coupler to characterize the RF system an estimate the compensation matrix for the static and dynamic errors. Like the first test, more than 1600 measurements must be done.

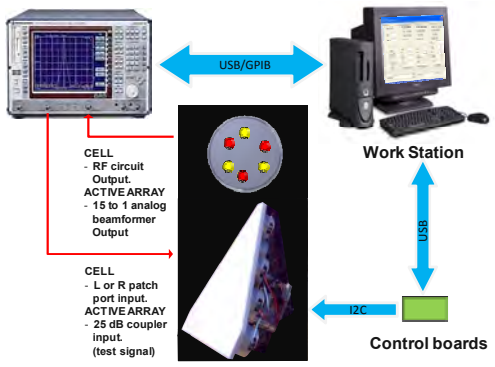

Fig. 4 S21 and the Test Signal measurement Setup

D. Anechoic chamber measurements

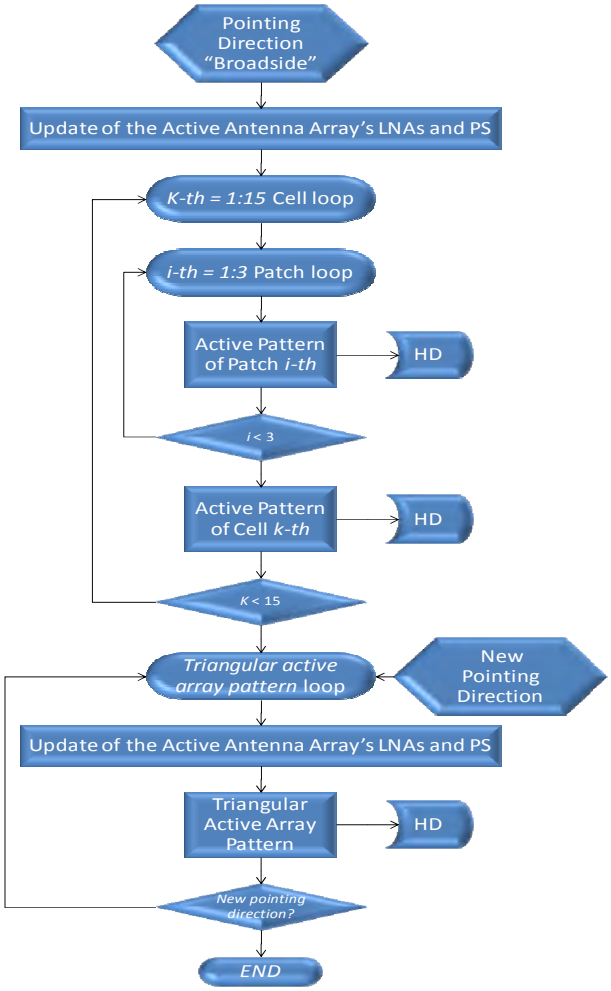

Fig. 5 Automated procedure for the anechoic chamber measurements

This is probably the most expensive and important stage of the measurements. Since this test needs almost 5 frequency and 61 measures per frequency to fulfil the selected On-site calibration model requirement, the anechoic chamber measurement takes more than 9 days nonstop work.

Thus, according to the exhaustive required measurement campaign, an efficient and scalable automated procedure depicted in Fig. 5 has been implemented to minimize operative costs and time. The anechoic chamber measurements setup is depicted Fig. 6.

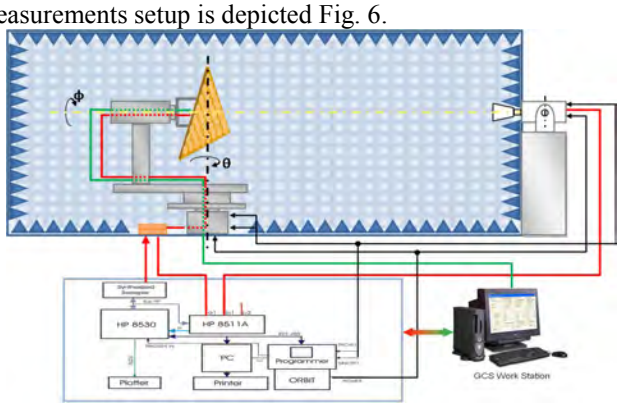

Fig. 6 Schematic representation of the spherical

V. Results

A set of measurements have been performed in the lab and in the anechoic chamber to complete the measurement procedure proposed in this work. The four groups of tests explained at section IV have been executed as a sequence and some of the more relevant results are presented in this discussion.

For the test A of the S21 parameter of the RF circuit, it was necessary to carried out 2430 measurements of the S21 parameter to evaluate the 6 states of the phase-shifters and 3 states of the LNA per patch. Results depicted in Fig. 7 and Fig. 8 have been performed to illustrate the standard deviation on the phase and gain of the RF circuits, respectively.

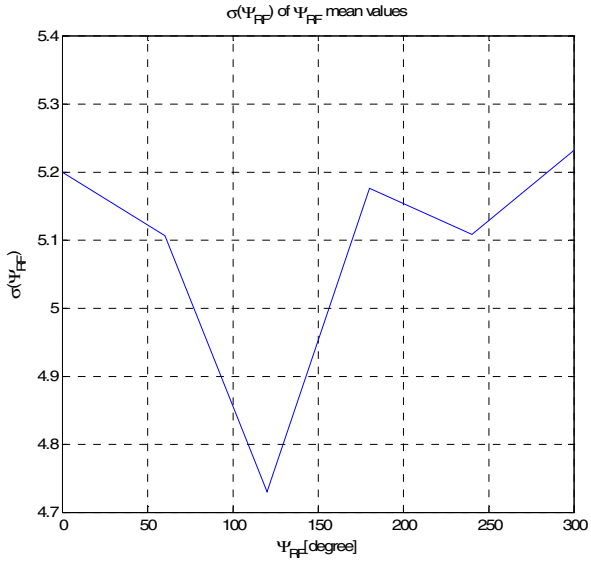

Fig. 7 Standard deviation (σ) of the Phase of the RF circuit as a function of the phase-shifter state

The standard deviation of the phase presented in Fig. 7 was obtained from the 5th cell of the triangular active array, and it is a measure of the dispersion from the phase average.

Furthermore, in Fig. 8 the standard deviation of the gain is shown. As previously, it is a measure of the dispersion from the gain average of the 5th cell of the triangular active array.

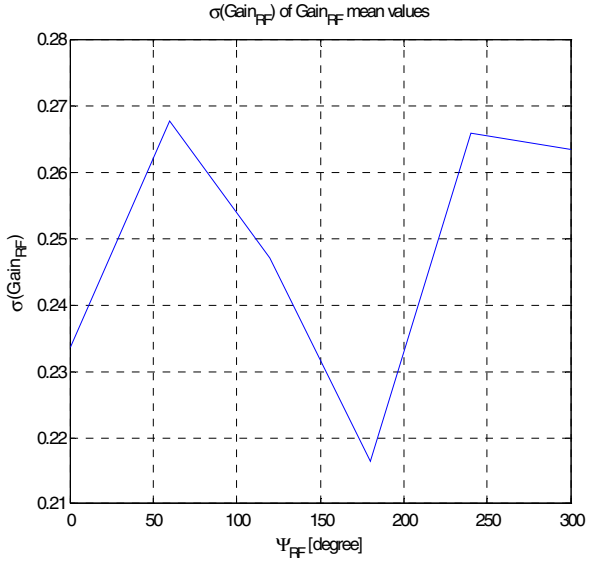

Fig. 8 Standard deviation (σ) of the Gain of the RF circuit as a function of the phase-shifter state

For the S coupling parameter test, it was applied a carefully measurement campaign to the radiating element's ports of the antenna array. The S coupling measured parameters were used in the simulation with the Pozar's active pattern model [6]. The Fig. 9 shows the errors in the pattern of the patch 1 due to the mutual coupling effect. The patch 1 is the element located at the upper corner of the triangular active array.

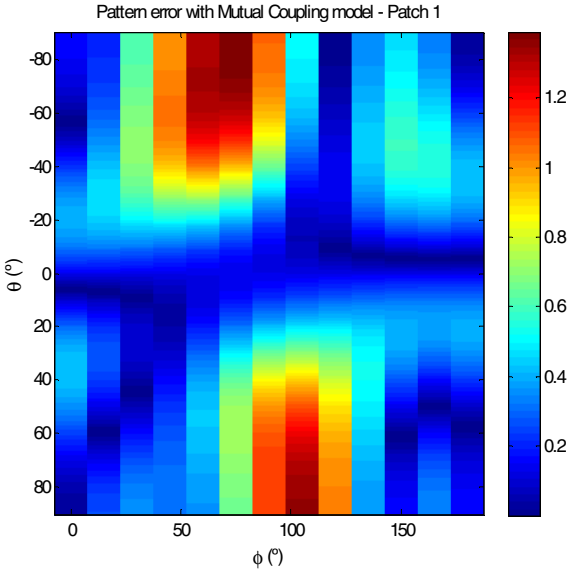

Fig. 9 Pattern errors due to the estimated mutual coupling effect of an element located at one corner

Besides, in order to show the behavioural of the mutual coupling effect as a function of the element location into the

array, Fig. 10 shows the errors in the pattern due to the mutual coupling of the central patch number 13.

It is important to separate in identically geometrical groups the elements in order to apply the mutual coupling model and compute the mutual coupling coefficients. Thus, the differences of the mutual coupling effect related to the element location are presented in this work.

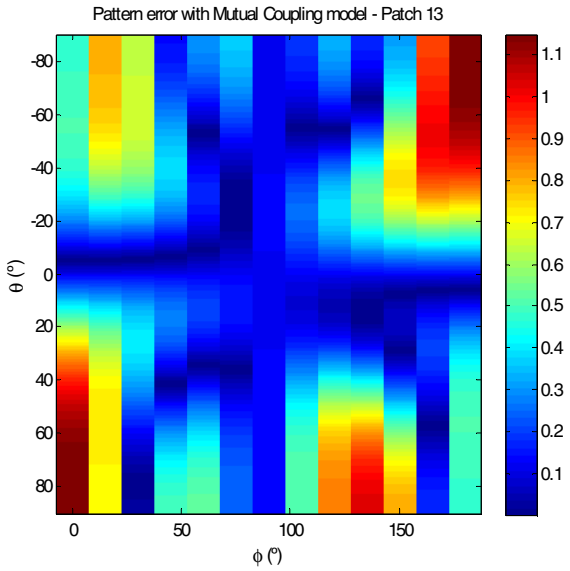

Fig. 10 Pattern errors due to the estimated mutual coupling effect of one central element

After the test C which is about the S21 measurements with the test signal, the compensation matrix of the RF circuit of the On-site calibration was obtained. The results of the amplitude and phase of the S21 parameter of the 5th Cell are depicted in Fig. 11 and Fig. 12, respectively. In contrast to the test A, the results of the test C include the weight of the the 15 to 1 signal combiner at the output of the triangular active array.

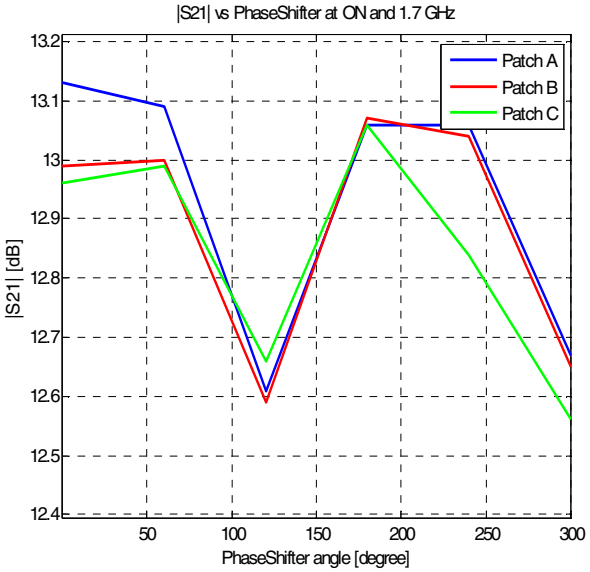

Fig. 11 |S21| measured with Test signal procedure

It is easy to signify the deviation in amplitude and phase values presented in the results.

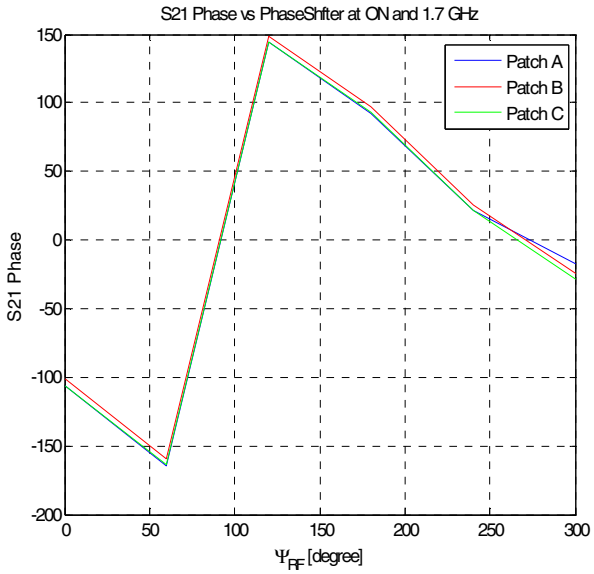

Fig. 12 S21 Phase measured with Test signal procedure

From the anechoic chamber measurement procedure are presented the measured pattern of the triangular active array and the active pattern of each patch of the cell 5.

The Fig. 13 depicts the normalized pattern of the triangular active array at theta = 30º, phi = 0º and f = 1.7 GHz, and the active array has a gain losses due to the miss-pointing about 1.5 dB.

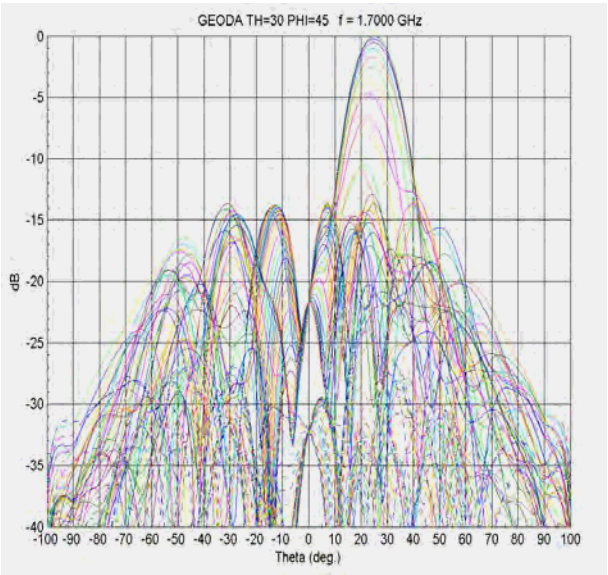

Fig. 13 Anechoic chamber measurement of the pattern of the triangular active array panel at Theta = 30º, Phi = 0º and f = 1.7 GHz.

The active pattern for the 45 patches were measured and the Fig. 14 presents the active pattern of the patches A,B and C of the Cell 5 at f = 1.7 GHz.

The pattern error due to the mutual coupling for cut φ = 90º and f = 1.7 GHz is depicted in Fig. 15. The mutual coupling effect is computed as the difference between the patch pattern

measured as a unique radiating element antenna and the active pattern of the patch of the active array.

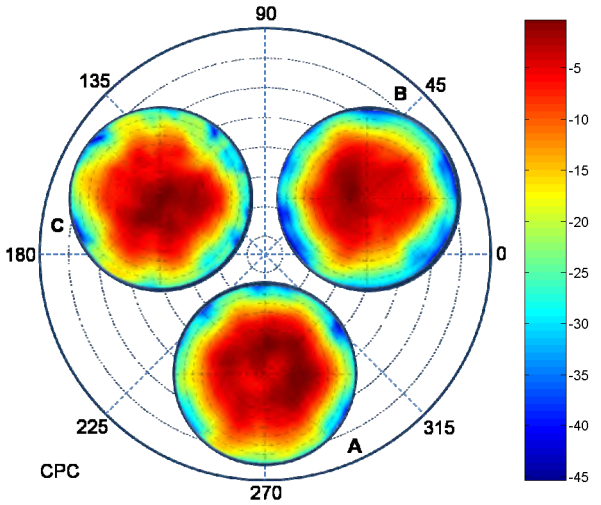

Fig. 14 Anechoic chamber measurement of the Active Pattern of the Cell 5, Patches A B C of the triangular active array panel at f = 1.7 GHz.

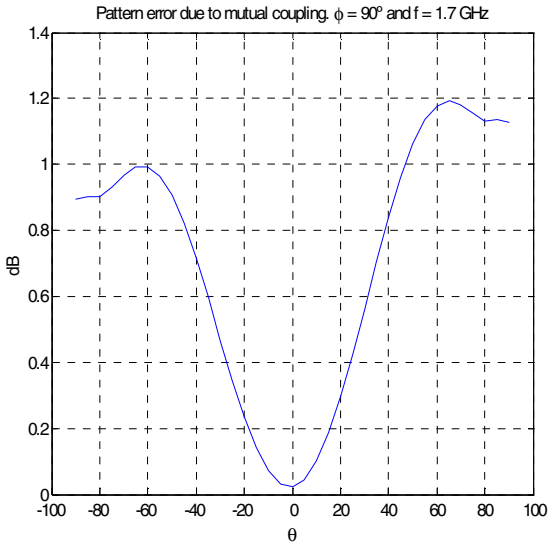

Fig. 15 Pattern errors due to the mutual coupling effect from measurement at patch 13, cut φ = 90º and f = 1.7 GHz.

The curve presented in the Fig. 15 is a 6 degree polynomial fitted curve of the resulting mutual coupling errors at φ = 90º and f = 1.7 GHz.

VI. Conclusions

In this work an automated measurement procedure for the calibration of planar active arrays is presented.

The characterization of the RF circuit has been done and its results support that the weight of the phase errors is higher than the weight of the gain errors of the RF circuits on the gain losses for miss-pointing due to its standard deviation.

The patch active pattern has been measured and contrasted with simulations, showing that the mutual coupling coefficient can be computed from measurement using the Pozar's mutual coupling model.

It is also demonstrated by simulation that it is important to separate in geometrical groups the elements in order to apply the mutual coupling model and compute the appropriate mutual coupling coefficients. The differences of the mutual coupling effect related to the element location of the array are presented in Fig. 9 and Fig. 10.

Furthermore, all the required data for the calibration process from measurement has been compiled and the compensation matrices for calibration have been computed, and the On-site calibration is modeled.

In addition, one automatic system scalable for future active antenna designs has been implemented in the anechoic chamber laboratory.

VII. Acknowledgment

Authors wish to thank MICINN (Ministerio de Ciencia e Innovación) and CICYT (Comisión Interministerial de Ciencia y Tecnología) for funding this work under the CROCANTE project (ref: TEC2008-06736/TEC).

References

[1] M. A. Salas Natera, R. Martínez Rodríguez-Osorio, Antón Sánchez, I. García-Rojo and L. Cuellar, "A3TB: Adaptive Antenna Array test-bed for tracking LEO satellites based on Software-Defined Radio," 59th International Austronautical Congress *IAC 2008*, Glasgow, October 2008, pp. 313-317.

[2] A. Torre, J. Gonzalo, R. M. Pulido, R. Martínez, "New Generation Ground Segment Architecture for LEO Satellites," 57th International Astronautical Congress *IAC 2006*, Valencia, October 2006.

[3] W. D. Ivancic, "Architecture and System Engineering Development Study of Space-Based Networks for NASA Missions," IEEE Aerospace Conference, Big Sky, 8-15 March 2003, pp. 1179-1186.

[4] M. Arias Campo, I. Montesinos Ortego, J. L. Fernández Jambrina and M. Sierra Pérez, "GEODA – GRUA: Diseño del módulo T/R," XXIV Simposium Nacional de la Unión Científica de Radio *URSI 2009*, Santander, 12 – 16 September 2009, pp. 115 - 116.

[5] M. Sierra Pérez, A. Torre, J.L. Masa, D. Ktorza and I. Montesinos, "GEODA: Adaptive Antenna Array for Metop Satellite Signal Reception," 4th ESA International Workshop on Tracking, Telemetry and Command System for Space Applications, Darmstadt, 11 - 14 September 2007.

[6] Pozar, D. M., "A relation between the active input impedance and the active element pattern of a phased array," IEEE Trans. On Antennas and Propagation, vol. 51, pp. 2486- 2489, Sept. 2003.